Chemistry and Materials

The Center for Science Innovation

Research Article

Chem. Mater. 4 (3) 2025, 107-116

Green design, synthesis, and characterization of a novel eight-membered silicon-boron-based cyclo-1,5-di(p-tolyl)-3,3,7,7-tetraphenyl-1,5-dibora-3,7-disiloxane, a Lewis acid, and its use for the adsorption of Fe^{3+} and Methylene blue from aqueous solution

Okpara Sergeant Bull*, Tubonimi Joseph Kio Ideriah, and Godstime Tamunofri Adirimo

Department of Chemistry, Rivers State University, Nkpolu-Oroworukwo, Port Harcourt, Private Mail Bag 5080, Nigeria

*Corresponding author: bull.okpara@ust.edu.ng

Received
19 August 2025

Received in revised form
21 September 2025

Accepted
07 October 2025

Published online
31 October 2025

DOI
https://doi.org/10.56425/cma.v4i3.115

Abstract

Metal ions such as Fe^{3+} and dye contamination such as methylene blue (MB) have caused environmental and health problems, particularly through industrial wastewater discharge. Some conventional treatment methods of removing these toxins are inefficient and unsustainable. Thus, this study focuses on the synthesis and characterization of cyclo-1,5-di(p-tolyl)-3,3,7,7-tetraphenyl-1,5-dibora-3,7-disiloxane, a Lewis acid, and its application in the adsorption of Fe^{3+} and MB from aqueous solution. The compound was synthesized via a condensation reaction between diphenylsilanediol (4.3 g, 19.97 mmol) and *p*-tolylboronic acid (2.72 g, 20.03 mmol) at reflux for 12 h. The crude product was recrystallized from petroleum ether yielding 2.89 g of blocky, colorless crystals (90% yield, melting point 260 °C). The compound was characterized using powder X-ray diffraction (PXRD) and fourier transform infrared (FT-IR) spectroscopy. Thereafter, the synthesized compound was used for the adsorption of Fe^{3+} and MB. The adsorption isotherms for both Fe^{3+} and MB follow the Freundlich with R^2 values of 0.8967 and 0.8769, respectively. These adsorption study results show the potential of the synthesized novel compound, as an adsorbent for the removal of Fe^{3+} and MB in aqueous solution, offering a promising future for application in wastewater treatment and environmental remediation.

Keywords: diphenylsilanediol, p-tolylphenylboronic acid, cyclodiborasiloxane, iron(III), methylene blue

1. Introduction

Numerous heavy metals (mostly cations) and dyes released into the environment by industrial production operations are causing a steady decline in water quality. These substances have been shown to be extremely hazardous and may persist in the aqueous environment [1]. Large-scale battery use, metal rinse procedures, fluidized bed bioreactors, pesticides, and the expansion of mining, rayon, tanning, textile, petrochemical, and paper manufacturing industries worldwide have all contributed to the steady increase in the concentration of heavy metals in wastewater. Wastewater tainted with heavy metals leaks into the environment, posing a threat to both the ecosystem and human health [2].

The problem of heavy metal contamination is spreading throughout the world. Although heavy metals are naturally occurring substances, excessive concentrations can be dangerous. Metals can enter the environment naturally or as a result of anthropogenic activities including mining, industrial manufacturing, and rubbish disposal [3]. Heavy metals can be dispersed and spread to neighbouring areas during windstorms or flooding, mining in particular poses a significant risk. Heavy metal contamination threatens both ecological and human health. These metals enter the

body through the food chain, where they can form hazardous compounds that damage cells [4].

About 9 billion tonnes of synthetic dyes are generated a year, and these have adverse effects on the ecosystem [5]. Dyes are coloured compounds that are widely used to colour things in the textile, printing, rubber, cosmetics, plastics, research laboratories, and leather sectors [6–8]. This leads to the generation of a large amount of coloured wastewater. They are frequently categorized as either non-ionic, cationic, or anionic dyes. The usage of dyes for fibre colouring is highest in the textile sector. These chemical dyes attach themselves to textiles or surface shells to impart colour. The textile and manufacturing sectors are expected to use over 10,000 commercially available dyes worldwide, with the textile sector consuming over 1000 tonnes annually. During the dyeing process, 10-15% of these dyes are released into wastewater as effluents [9]. By blocking light through chromogenic functional groups, decreasing photosynthesis in aquatic plants and algae, and hindering the vital processes of other aquatic organisms, this damages aquatic species [8–9].

Specifically, the synthetic, heterocyclic aromatic, cationic chemical molecule known as methylene blue (MB), $C_{16}H_{18}ClN_3S$, has a molar mass of 319.85 g/mol. MB is widely used as a colourant in cotton, textiles, food, cosmetics, temporary hair colourants, wool, silk, paper, and pharmaceuticals [10]. This common cationic dye is dangerous, mutagenic, carcinogenic, and environmentally persistent. Serious health consequences from extended exposure to MB include anaemia, cancer, nausea, vomiting, ocular irritation, methemoglobinemia, and mental health problems [11]. For this reason, wastewater containing heavy metals or dyes needs to be cleaned before being released into the environment to guarantee its safe discharge. Numerous remediation procedures, including biological and physicochemical methods, have been developed [12]. Adsorption has been regarded as one of the most efficient means for the removal of heavy metals and dyes from wastewater due to its several advantages, which include its low cost, adaptability, and high efficacy [1]. Due to its ease of use, broad applicability, high removal rate, and low cost of reuse, adsorption is the most promising method that has been thoroughly investigated for removing heavy metal ions from wastewater [2].

Traditional adsorbents such as clays, zeolites, and activated carbons have been widely used for the removal of dyes and heavy metals [13]. These have, however, had a number of disadvantages, such as the incapacity to use their microporosity for the synthesis of large molecules and the high susceptibility of zeolites to deactivation through steric blocking of heavy secondary products or irreversible adsorption [14]. Commercial activated carbon is now thought to be the best carbonaceous adsorbent; yet, its utility has been severely constrained by its high production costs [4]. In addition, activated carbon has an unpredictable pore size, poor adsorption performance, high ash content, low sphericity, and low mechanical strength. The primary obstacle to the widespread use of activated carbon in industry is its high cost of manufacturing, which is caused by the price of the raw materials, chemicals, and energy employed [15]. Many adsorbents have also been made from biomass, however, in order to improve adsorption adequacy, these typically need to undergo pretreatment procedures [16].

According to Gilbert Lewis, an atom, ion, or molecule that has an empty, unoccupied, or unfilled atomic or molecular orbital that can take in or admit an electron pair is referred to as a Lewis acid. This suggests that Lewis acids are compounds with partial or unfulfilled octets. An electron pair from the Lewis base's highest occupied molecular orbital (HOMO) is donated to the Lewis acid's lowest unoccupied molecular orbital (LUMO) by the Lewis base, also known as an electron pair donor. In short, a Lewis acid is an acid that takes in pairs of electrons.

Among the various Lewis acids investigated over the last two decades, those containing boron and other group 13 elements have been found attractive for their unique bonding properties, interactions with transition metals, low cost, and being benign to the environment [17]. Recent breakthroughs in materials science have resulted in the creation of nanostructured adsorbents, such as carbon nanotubes and graphene, with improved adsorption properties [18].The use of silicon (Si) and boron (B) in Lewis acid frameworks provides distinct advantages for metal ion adsorption and catalysis. Si atoms improve thermal and chemical stability, whereas B serves as an active metal binding site [19]. The combination of Si and B in bidentate Lewis acids, such as o-(silyl)(boryl)benzenes, results in very stable structures with variable Lewis acidity [20]. Lewis acidic centers in materials such as Metal-Organic Frameworks (MOFs) and boron-containing compounds have demonstrated considerable potential for heterogeneous catalysis and water purification [21]. B derivatives are Lewis acids par excellence because the central boron atom lacks electrons and has an empty *p*-orbital [22]. Boron-based Lewis acid complexes have emerged as a viable bifunctional catalyst for a variety of processes, including environmental ones. These complexes may act as both electron acceptors and donors, making them useful for selective adsorption of metal pollutants [23]. norganic cyclic systems like borasiloxanes (B-O-Si)

have a wide range of applications due to their attractive properties, including unique magnetic and optical behavior, electronic structures, and potential quasi-aromatic character [24].

Borasiloxanes, which are composed of alternating silicon and boron atoms, have been intensively researched for their chemical stability and reactivity. These molecules are both Lewis acidic and flexible, making them useful for catalysis and other applications [25]. The second most prevalent element in the crust of the Earth is silicon. It is frequently found in nature, especially in quartz, silicates, and other minerals. A bigger atomic size, the capacity to construct intricate extended structures, and a variety of oxidation states are some of the unique features of silicon chemistry, despite certain parallels with carbon chemistry. Because of these distinctions, silicon chemistry has a distinct character and is an intriguing field of study with applications in catalysis, materials science, and other fields [26]. On the other hand, Boron is a group 13 metalloid element that has chemical characteristics similar to carbon and silicon, albeit with less electrons. Boron, which was first separated in 1808, is relatively rare in the Earth's crust but can be found in minerals such as borax and kernite. The use of silicon (Si) and boron (B) in lewis acid frameworks provide distinct advantages for metal ion adsorption and catalysis. Silicon atoms can improve thermal and chemical stability, and B serves as an active metal binding site [19]. The combination of silicon and boron in bidentate Lewis acids, such as o-(silyl)(boryl)benzenes, results in very stable structures with variable Lewis acidity [20].

Lewis acidic centers in materials like Metal-Organic Frameworks (MOFs) and boron containing compounds have demonstrated significant potential for heterogeneous catalysis and water purification [27]. Transannular interactions between boron and silicon/germanium atoms can be used to modify the Lewis acidity of cage-shaped borates [19]. Diphenylsilanediol, phenylboronic acid, and molecular sieves for water removal have all been used in the literature to synthesize cyclo-1,3,3,5,7,7-hexaphenyl-1,5-dibora-3,7-disiloxane ($Ph_6B_2Si_2O_4$), with a stated compound yield of 87% [28–30]. However, the water was eliminated in the current investigation using molecular sieves.

Cyclo-Silicon-boron-based Lewis acid complexes have emerged as a viable bifunctional catalyst for a variety of processes, including environmental ones [29,31]. These complexes may act as both electron acceptors and donors, making them useful for selective adsorption of metal pollutants [32]. Inorganic cyclic systems, such as borasiloxanes (B-O-Si), are highly attractive in appearance and serve as important systems with a wide range of applications due to their fascinating magnetic and optical properties, electronic structures, potential quasi-aromatic character, and the ability to form extended π-π intra and intermolecular interactions [23,27,28]. Metal ions, such as Fe^{3+}, and dye contamination have caused environmental and health problems, particularly through industrial wastewater discharge [31,32]. With their customizable catalytic characteristics, silicon-boron-based Lewis acids offer a promising option. The purpose of this study is to synthesize and characterize cyclo-1,5-di(*p*-tolyl)-3,3,7,7-tetraphenyl-1,5-dibora-3,7-disiloxane, as well as evaluate its efficacy in the adsorption of Fe^{3+} ions and MB from aqueous solution.

2. Materials and Methods

2.1. Materials

All chemicals and reagents (diphenylsilanediol, tolylboronic acid, toluene, petroleum ether, $Fe(NO_3)_3.9H_2O$, methylene blue (MB), used in this work were commercially sourced and of analytical grade. They were used without further purification except otherwise stated. Molecular sieves (1.6 mm rods, 0.4 nm pores) were preheated in the oven before use.

2.2. Methods

2.2.1. Synthesis of cyclo-1,5-di(p-tolyl)-3,3,7,7-tetraphenyl-1,5-dibora-3,7-disiloxane Lewis Acid (3)

In a round bottom flask containing preheated molecular sieves, 150 mL of toluene and magnetic stirrer bar, 4.32 g (19.97 mmol) of diphenylsilanediol and 2.72 g (20.03 mmol) of *p*-tolylphenylboronic acid was added and stirred at reflux for 12 h as shown in Fig 1. Thereafter, the mixture and its content was allowed to cool to room temperature. Following this, the mixture was filtered and the filtrate collected. The filtrate was concentrated under reduced pressure with the use of a rotary evaporator to give colourless crude product. The crude product was recrystallized from petroleum ether, giving clean colourless crystals of cyclo-1,5-di(*p*-tolyl)-3,3,7,7-tetraphenyl-1,5-dibora-3,7-disiloxane after 24 h at 90% yield. The resulting crystals were characterized by melting point (260 °C), fourier transform infrared (FT-IR) spectroscopy and powder X-ray diffraction (PXRD).

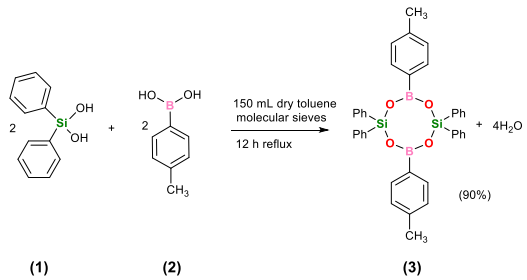

Figure 1. *Synthesis of cyclo-1,5-di(p-tolyl)-3,3-7,7-tetraphenyl-1,5-dibora-3,7-disiloxane.*

2.2.2. Adsorption studies for iron

A stock solution of Fe^{3+} was prepared from Fe $(NO_3)_3.9H_2O$ with molar mass of 404.06g/mol.

% of Fe in Fe $(NO_3)_3.9H_20 = \frac{55.85}{404.6}$ x 100 = 13.82%

The mass of Fe $(NO_3)_3.9H_2O$ salt required for the preparation of the stock solution containing 1000mg/L of Fe^{3+} ions is 1000/0.1382 = 7236 mg/L = 7.236g of $Fe(NO_3)_3.9H_2O$.

7.236 g of Fe $(NO_3)_3.9H_2O$ was weighed into a 1000 mL volumetric flask and dissolved in distilled water up to the 1 L mark of the volumetric flask. Diluted solutions of 10 mg/L, 20 mg/L, 30 mg/L, 40 mg/L, 50 mg/L, 60 mg/L, 70 mg/L, 80 mg/L, 90 mg/L, 100 mg/l, 110 mg/L and 120 mg/L were prepared from this solution using the formula:

$C_1V_1 = C_2V_2$ (1)

Where C1 = concentration of stock solution, V_1 = volume of stock solution needed, C_2 = desired concentration after dilution, V_2 = final volume after dilution

The solutions were poured into 100 mL containers, each containing 0.1 g of the synthesized crystals and labeled accordingly with the pH of each adjusted to 6 using a pH meter to ensure optimal adsorption. These containers were then placed on an orbital shaker and agitated for 3 h at 220 rotation per minute (rpm). After 3 h, the mixtures were filtered and the filtrate sent for atomic absorption spectroscopy (AAS) analysis to determine the final concentrations of the solutions.

2.2.3. Adsorption studies for MB

1 g of dry MB powder was weighed and dissolved in a 1000 mL volumetric flask. The solution was stirred to ensure the MB was properly dissolved and the more distilled water was added up to the 1 L mark. This served as the stock solution which was further diluted into lower concentrations.

The diluted solutions of 10 mg/L, 20 mg/L, 30 mg/L, 40 mg/L, 50 mg/L, 60 mg/L, 70 mg/L, 80 mg/L, 90 mg/L and 100 mg/L were gotten from this solution using the formula:

$C_1V_1 = C_2V_2$ (2)

The mixtures were put into 100 mL containers, each containing 0.1 g of the synthesized crystals and labeled accordingly with the pH of each adjusted to 6 using a pH meter to ensure optimal adsorption. These containers were then placed on an orbital shaker and agitated for 3 h at 220rpm. After 3 h, the mixture was filtered and the filtrate sent for Ultraviolet-Visible spectroscopy to determine the final concentrations of the solutions.

The adsorption isothermal process is carried out to describe the adsorption process between adsorbents and adsorbates. This isotherm modeling is carried out based on two models, namely: the Langmuir isotherm and the Freundlich isotherm. Langmuir's isotherm describes the process of monolayer adsorption, where each active site can only absorb one waste molecule. The equation of Langmuir's isotherm (Equation 3) [35].

$\frac{1}{Qm} = \frac{1}{K.Qm} \times \frac{1}{Ce} \times \frac{1}{Qm}$ (3)

Where Ce is the concentration of adsorbates in equilibrium, Qe is the amount of adsorbate absorbed in equilibrium, K is the Langmuir constant, and Qm is the adsorption capacity [10].

The Freundlich isotherm model describes the multilayer adsorption process, where each active site of the adsorbent has different adsorption capabilities so that it can form a multilayer in its interaction between adsorbent and adsorbate. Here is Freundlich's isotherm equation (Equation 3-4) [35].

$Qe = K.\ Ce^n$ (4)

$\text{Log } Qe = \frac{1}{n} \text{ x log } Ce + \text{Log } K$ (5)

Where Qe is the number of adsorbates that are absorbed, Ce is the equilibrium concentration, K and n are constants [7].

3. Results and Discussion

Colourless block-like-shaped crystalline solids of cyclo-1,5-di(*p*-tolyl)-3,3,7,7-tetraphenyl-1,5-dibora-3,7-disiloxane ($Ph_6B_2Si_2O_4Me_2$) were obtained with an actual yield of 3.21 g (Fig 2).

Figure 2. Colourless crystals of cyclo-1,5-di(p-tolyl)-3,3,7,7-tetraphenyl-1,5-dibora-3,7-disiloxane ($Ph_6B_2Si_2O_4Me_2$).

The FT-IR spectrum of diphenylsilanediol in Fig 3 revealed high absorption peaks at 3232 cm^{-1} (O-H), 1208.9 cm^{-1} (Si-C), 3071.268 cm^{-1} (C-H), and 1225 cm^{-1} (Si-O), indicating its chemical structure. These findings are comparable with similar peaks observed by Jiang *et al.*, (2015) in their investigation of diphenylsilanediol and Tagliazucca *et al.*, (2011) in their analysis of silsesquioxanes, demonstrating the compound's stable structure.

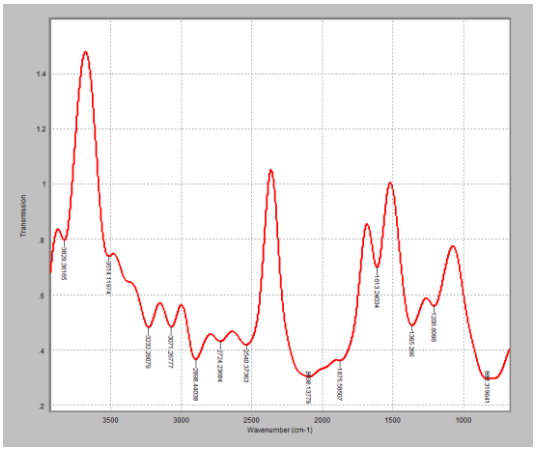

Figure 3. FT-IR spectrum of diphenylsilanediol.

The FT-IR spectrum of *p*-tolylboronic acid in Fig 4 showed absorption peaks at 1195 cm^{-1} (B-O), 3120 cm^{-1} (C-H), and 1451 cm^{-1} (C=C) [34,35] found similar B-O stretching vibrations at 1299 cm^{-1} in their investigation of boronic acids [38] also validated the presence of *p*-tolyl groups in the boronic acid structure [36,37] observed comparable absorption patterns in their FT-IR investigation of borasiloxane compounds. Both FT-IR spectra of the starting materials showed broad and strong absorption bands in the region 3200-3600 cm^{-1} indicating the presence of O-H groups.

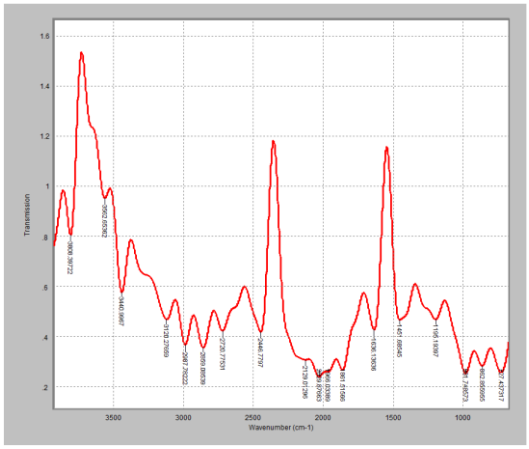

Figure 4. FT-IR spectrum of p-tolylboronic acid.

However, the FT-IR spectrum of the newly formed cyclo-1,5-di(*p*-tolyl)-3,3,7,7-tetraphenyl-1,5-dibora-3,7-disiloxane (Fig 5) confirmed the presence of significant absorption peaks at 2987 cm^{-1} (C-H), 1402 cm^{-1} (B-O), 1312 cm^{-1} (Si-C), and 1131 cm^{-1} (Si-O). It was observed that the broad O-H peaks characteristic of the starting materials is absent, indicating that the formation of a new compound. These findings are congruent with those of [39], who found similar bands in their analyses of cyclic borasiloxane compounds. [18,39] also synthesized silicon and germanium-based borates and found similar IR absorption patterns.

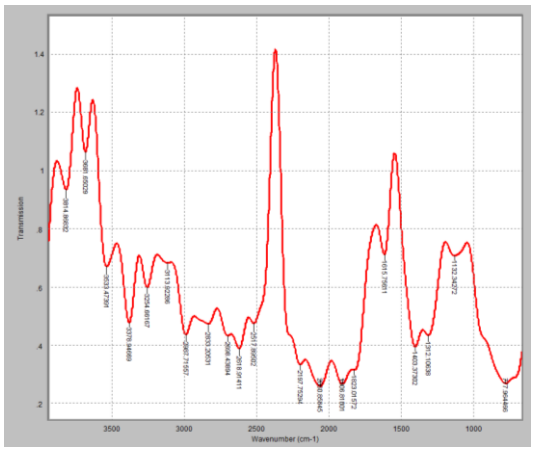

Figure 5. FT-IR spectrum of cyclo-1,5-di(p-tolyl)-3,3,7,7-tetraphenyl-1,5-dibora-3,7-disiloxane.

In addition, the crystallinity of the synthesized cyclo-1,5-di(p-tolyl)-3,3,7,7-tetraphenyl-1,5-dibora-3,7 disiloxane was confirmed with a powder X-ray diffraction study as shown in Fig 6. The peaks at 2θ values of 36.5°, 39°, 43.5°, 45° and 50.5° have intensities of 100, 150, 1150, 130, and 800 counts respectively. The peak at 43.5° has the highest intensity, suggesting a strong reflection. The presence of multiple peaks indicates a crystalline material [42,43].

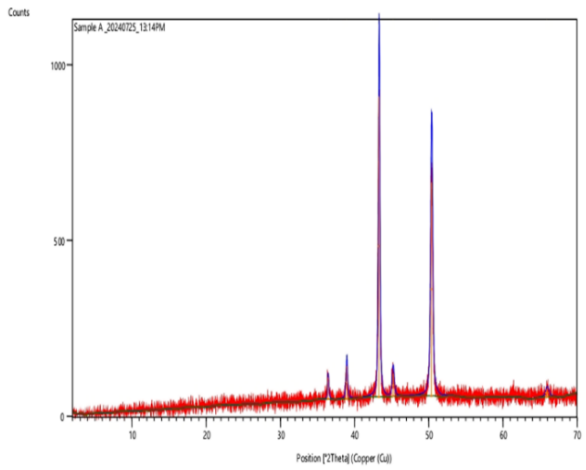

Figure 6. X-ray diffraction of cyclo-1,5-di(p-tolyl)-3,3,7,7-tetraphenyl-1,5-dibora-3,7-disiloxane.

Adsorption experiments (Table 1) revealed a high Fe^{3+} removal efficiency of 95.4% to 99.9%, with adsorption capacity progressively rising from 4.98 mg/g to 59.9 mg/g, and a removal efficiency of 60.3% to 96.8% for MB as shown in Table 2.

Table 1. Adsorption efficiency for Fe^{3+}.

Co (mg/L)	Ce (mg/L)	Co-Ce (mg/L)	Qe (mg/g)	%Fe^{3+}
10	0.0485	9.95	4.98	99.5
20	0.0024	19.99	9.99	99.9
30	0.0307	29.97	14.98	99.9
40	0.1563	39.84	19.92	99.6
50	0.0035	49.99	24.99	99.9
60	0.1923	59.81	29.90	99.7
70	3.2133	66.79	33.39	95.4
80	0.0013	79.99	39.99	99.9
90	3.8737	86.13	43.06	95.7
100	0.0030	99.99	49.99	99.9
110	0.0006	109.99	54.99	99.9
120	0.0004	119.99	59.99	99.9

This is consistent with previous adsorption experiments, which have shown that the presence of Lewis acid sites on the adsorbent improves metal ion and dye binding. The high adsorption capacity is due the electron-deficient boron atoms as well as the silicon atoms with vacant *d*-orbitals to accept pairs of electrons, thereby acting as enhanced active sites for the complexation and adsorption of Fe^{3+} and MB. From the isotherm modeling, the adsorption of both Fe^{3+} and MB follow the Freundlich isotherm as their R^2 value is closer to unity when compared to that of Langmuir model. The adsorption process follows the principles of Lewis acid-base interactions, where Fe^{3+} and MB, acting as Lewis acids, engage with the electron-deficient silicon and boron centers, which act as Lewis bases.

Table 2. Adsorption efficiency for MB.

Co (mg/L)	Abs	Ce (mg/L)	Co-Ce	Qe (mg/g)	%MB
10	1.047	3.97	6.03	3.02	60.3
20	0.169	0.64	19.36	9.68	96.8
30	1.952	7.38	22.62	11.31	75.4
40	2.333	8.86	31.14	15.57	77.9
50	2.401	9.12	40.88	20.44	81.8
60	2.798	10.62	49.38	24.9	82.3
70	2.526	9.56	60.44	30.22	86.3
80	2.674	10.14	69.86	34.93	87.3
90	2.787	10.59	79.41	39.71	88.3
100	2.857	10.84	89.16	44.58	89.2

3.2 Adsorption Isotherms

The adsorption isotherm model is crucial in understanding the relationship between the amount of adsorbate adsorbed by the adsorbent surface and the adsorbate concentration at equilibrium. This relationship helps to describe the interaction between molecules or ions and the active sites on the adsorbent surface. To determine the best-fit isotherm model, we used data from optimized adsorption conditions. The Langmuir model assumes a homogeneous surface, while the Freundlich model assumes a heterogeneous surface.

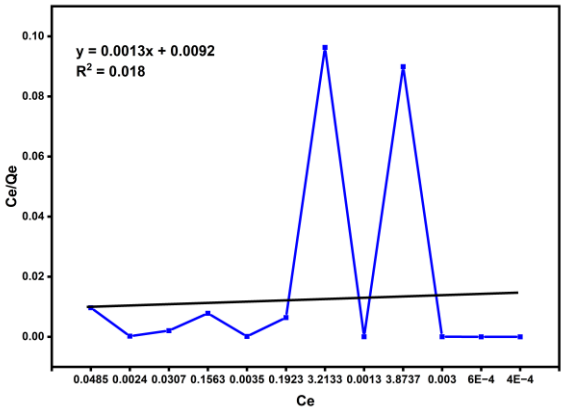

Figure 7. Langmuir adsorption isotherm for Fe^{3+} in aqueous solution using cyclo-1,5-di(p-tolyl)-3,3,7,7-tetraphenyl-1,5-dibora-3,7-disiloxane

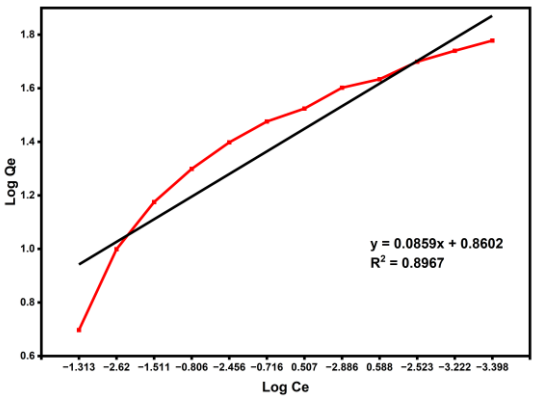

Figure 8. Freundlich adsorption isotherm for Fe^{3+} in aqueous solution using cyclo-1,5-di(p-tolyl)-3,3,7,7-tetraphenyl-1,5-dibora-3,7-disiloxane.

For F^{3+} adsorption, the isotherm curves for Langmuir and Freundlich models are presented in Fig 7 and Fig 8, respectively. Based on the R-squared values, the Freundlich model (R^2 = 0.8967) provided a better fit than the Langmuir model (R^2 = 0.018). This model accounts for the exponential distribution of active sites and their energies, describing a multilayer adsorption system. This implies that the cyclo-1,5-di(p-tolyl)-3,3,7,7-tetraphenyl-1,5-dibora-3,7-disiloxane adsorbent involves multilayer adsorption on a heterogeneous surface. The Freundlich model assumes that the heat of adsorption is not evenly distributed on a heterogeneous surface, thus giving room for multilayer adsorption. This multilayer adsorption leads to higher adsorption capacities. Additional implication of the better fit of the Freundlich model as against the Langmuir model is that the adsorption mechanism is more complex than a mere simple monolayer adsorption,

involving multiple layers, and interactions between the adsorbate and adsorbent [44,45]. Similarly, for MB adsorption, the Freundlich model (R^2 = 0.8769) outperforms the Langmuir model (R^2 = 0.3321), as shown in Fig 10 and Fig 9, respectively.

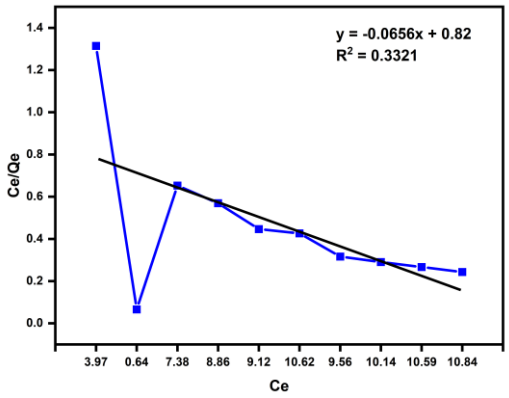

Figure 9. Langmuir adsorption isotherm for MB in aqueous solution cyclo-1,5-di(p-tolyl)-3,3,7,7-tetraphenyl-1,5-dibora-3,7-disiloxane.

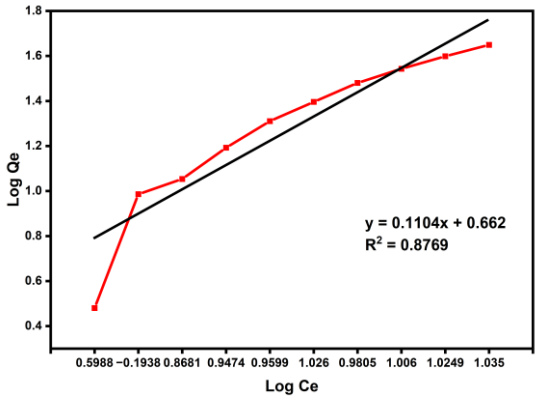

Figure 10. Freundlich adsorption isotherm for MB in aqueous solution cyclo-1,5-di(p-tolyl)-3,3,7,7-tetraphenyl-1,5-dibora-3,7-disiloxane.

These results suggest that the adsorption of F^{3+} and MB onto the synthesized adsorbent occurs through multilayer adsorption on a heterogeneous surface rather than monolayer on a homogeneous surface.

4. Conclusion

Cyclo-1,5-di(*p*-tolyl)-3,3,7,7-tetraphenyl-1,5-dibora 3,7-disiloxane was successfully synthesized via a [2+2] cyclocondensation reaction of diphenylsilanediol and p-tolylphenylboronic acid using dry toluene as solvent at reflux and activated molecular sieves as water sorbent. The crude was crystallized from petroleum ether and characterized using melting point, FT-IR spectroscopy and PXRD with a notable yield of 90.14%. The characterization results show the formation of the desired product with respect to literature [25,30,39,40,43,46,47]. The adsorbent effectively adsorbed Fe^{3+} and MB from aqueous solution. The adsorption isotherms for both Fe^{3+} and MB were better described by the Freundlich model, as the R^2 values were closer to unity than those for the Langmuir model. Thus, it can be concluded that cyclo-1,5-di(p-tolyl)-3,3,7,7-tetraphenyl-1,5-dibora-3,7-disiloxane is an effective adsorbent for the removal of Fe^{3+} and MB from wastewater.

Author contributions

Okpara Sergeant Bull: conceptualization, methodology, software, validation, formal analysis, investigation, resources, data curation, writing - original draft, writing - review & editing, visualization, funding acquisition, supervision, project administration. **Tubonimi Joseph Kio Ideriah**: conceptualization, validation, data curation, writing - review & editing, supervision, project administration. **Godstime Tamunofri Adirimo**: methodology, investigation, resources, writing - original draft.

Conflicts of interest

The author declares that there is no conflict of interest.

Acknowledgement

The financial support given by the Nigerian Government through the Petroleum Technology Development Fund (PTDF), the Tertiary Education Trust Fund (TETFUND), and the Rivers State University, Port Harcourt, Nigeria as well as that from Chief Abbiyesuku, Abbi Faithful are graciously acknowledged.

References

[1] T. Zhang, W. Wang, Y. Zhao, H. Bai, T. Wen, S. Kang, G. Song, S. Song, S. Komarneni, Removal of heavy metals and dyes by clay-based adsorbents: From natural clays to 1D and 2D nano-composites, *Chemical Engineering Journal*. **420** (2021) 127574. https://doi.org/https://doi.org/10.1016/j.cej.2020.127574.

[2] N.A.A. Qasem, R.H. Mohammed, D.U. Lawal, Removal of heavy metal ions from wastewater: a comprehensive and critical review, *Npj Clean Water*. **4** (2021). https://doi.org/10.1038/s41545-021-00127-0.

[3] S. Mitra, A.J. Chakraborty, A.M. Tareq, T. Bin Emran, F. Nainu, A. Khusro, A.M. Idris, M.U. Khandaker, H. Osman, F.A. Alhumaydhi, J.S.-G. Simal-Gandara, Impact of heavy metals on the environment and human health: Novel therapeutic insights to counter the toxicity, *Journal of King Saud University - Science*. **34** (2022) 101865. https://doi.org/https://doi.org/10.1016/j.jksus.2022.101865.

[4] V. Singh, G. Ahmed, S. Vedika, P. Kumar, S.K. Chaturvedi, S.N. Rai, E. Vamanu, A. Kumar, Toxic heavy metal ions contamination in water and their sustainable reduction by eco-friendly methods: isotherms, thermodynamics and kinetics study, *Scientific Reports*. **14** (2024) 1–13. https://doi.org/10.1038/s41598-024-58061-3.

[5] B. Lellis, C.Z. Fávaro-Polonio, J.A. Pamphile, J.C. Polonio, Effects of textile dyes on health and the environment and bioremediation potential of living organisms, *Biotechnology Research and Innovation*. **3** (2019) 275–290. https://doi.org/https://doi.org/10.1016/j.biori.2019.09.001.

[6] V.B. Mane, S. Benkar, S. Bhavsar, A. Bandhankar, Removal of Dye From Wastewater Using Agricultural Waste As Low, *Journal of Emerging Technologies and Innovative Research*. **7** (2020) 404–414.

[7] Y. Pratiwi, M. Aulia, B.A. Riyandari, D.N. Anisa, Methylene Blue Adsorption using Magnetite-Modified Tea Waste Adsorbent, *Chemistry and Materials*. **4** (2025) 58–65. https://doi.org/https://doi.org/10.56425/jr1w4h95.

[8] F. Mahdavi, S. Yousef Ebrahimipour, S. Mohammad Ali Hosseini, R. Shaghaghian, S. Jamiladin Fatemi, S. Ramezanpour, M. Mohamadi, Synthesis and application of gadolinium-doped ZnO/silica mesoporous nanocomposite for methylene blue removal, *Journal of Molecular Structure*. **1318** (2024) 139175. https://doi.org/https://doi.org/10.1016/j.molstruc.2024.139175.

[9] R.V. Kandisa, N. Saibaba KV, Dye Removal by Adsorption: A Review, *Journal of Bioremediation & Biodegradation*. **07** (2016). https://doi.org/10.4172/2155-6199.1000371.

[10] J. Fito, M. Abewaa, A. Mengistu, K. Angassa, A.D. Ambaye, W. Moyo, T. Nkambule, Adsorption of methylene blue from textile industrial wastewater using activated carbon developed from Rumex abyssinicus plant, *Scientific Reports*. **13** (2023) 1–17. https://doi.org/10.1038/s41598-023-32341-w.

[11] M. Ismail, K. Akhtar, M.I. Khan, T. Kamal, M.A. Khan, A. M. Asiri, J. Seo, S.B. Khan, Pollution, Toxicity and Carcinogenicity of Organic Dyes and their Catalytic Bio-Remediation, *Current Pharmaceutical Design*. **25** (2019) 3645–3663. https://doi.org/10.2174/1381612825666191021142026.

[12] P. Zhang, M. Yang, J. Lan, Y. Huang, J. Zhang, S. Huang, Y. Yang, J. Ru, Water Quality Degradation Due to Heavy Metal Contamination: Health Impacts and Eco-Friendly Approaches for Heavy Metal Remediation, *Toxics*. **11** (2023). https://doi.org/10.3390/toxics11100828.

[13] A. Gopalakrishnan, R. Krishnan, S. Thangavel, G. Venugopal, S.-J. Kim, Removal of heavy metal ions from pharma-effluents using graphene-oxide nanosorbents and study of their adsorption kinetics, *Journal of Industrial and Engineering Chemistry*. **30** (2015) 14–19. https://doi.org/https://doi.org/10.1016/j.jiec.2015.06.005.

[14] A. Chakraborty, A. Pal, B.B. Saha, A Critical Review of the Removal of Radionuclides from Wastewater Employing Activated Carbon as an Adsorbent, *Materials*. **15** (2022). https://doi.org/10.3390/ma15248818.

[15] M.C. Silva, L. Spessato, T.L. Silva, G.K.P. Lopes, H.G. Zanella, J.T.C. Yokoyama, A.L. Cazetta, V.C. Almeida, H3PO4–activated carbon fibers of high surface area from banana tree pseudo-stem fibers: Adsorption studies of methylene blue dye in batch and fixed bed systems, *Journal of Molecular Liquids*. **324** (2021) 114771. https://doi.org/https://doi.org/10.1016/j.molliq.2020.114771.

[16] R. Agarwala, L. Mulky, Adsorption of Dyes from Wastewater: A Comprehensive Review, *ChemBioEng Reviews*. **10** (2023) 326–335. https://doi.org/10.1002/cben.202200011.

[17] H. Fang, M. Oestreich, Defunctionalisation catalysed by boron Lewis acids, *Chemical Science*. **11** (2020) 12604–12615. https://doi.org/10.1039/d0sc03712e.

[18] A. Hussain, S. Madan, R. Madan, Removal of Heavy Metals from Wastewater by Adsorption, in: M.K. Nazal, H. Zhao (Eds.), Heavy Metals, IntechOpen, Rijeka, 2021. https://doi.org/10.5772/intechopen.95841.

[19] A. Konishi, K. Nakaoka, H. Nakajima, K. Chiba, A. Baba, M. Yasuda, Tuning Lewis Acidity by a Transannular pπ–σ* Interaction between Boron and Silicon/Germanium Atoms Supported by a Cage-Shaped Framework, *Chemistry – A European Journal*. **23** (2017) 5219–5223. https://doi.org/https://doi.org/10.1002/chem.201700659.

[20] J. Shimada, A. Tani, C. Hanazato, T. Masuyama, Y. Yamamoto, A. Kawachi, Synthesis of B/Si Bidentate Lewis Acids, o-(Fluorosilyl)borylbenzenes and o-(Difluorosilyl)borylbenzenes, and Their Fluoride Ion Affinities, *ACS Omega*. **7** (2022) 30939–30953. https://doi.org/10.1021/acsomega.2c02775.

[21] Z. Hu, D. Zhao, Metal–organic frameworks with Lewis acidity: synthesis{,} characterization{,} and catalytic applications, *CrystEngComm*. **19** (2017) 4066–4081. https://doi.org/10.1039/C6CE02660E.

[22] I.B. Sivaev, V.I. Bregadze, Lewis acidity of boron compounds, *Coordination Chemistry Reviews*. **270**–

271 (2014) 75–88. https://doi.org/https://doi.org/10.1016/j.ccr.2013.10.017.

[23] Y. Li, J. Zhang, S. Shu, Y. Shao, Y. Liu, Z. Ke, Boron-Based Lewis Acid Transition Metal Complexes as Potential Bifunctional Catalysts, *Chinese Journal of Organic Chemistry*. **37** (2017) 2187–2202. https://doi.org/10.6023/cjoc201703002.

[24] P.V.V.N. Kishore, V. Baskar, Twelve-membered B2Si4O6 borasiloxane macrocycles, *Journal of Organometallic Chemistry*. **743** (2013) 83–86. https://doi.org/10.1016/j.jorganchem.2013.06.036.

[25] O.S. Bull, C. Don-Lawson, Facile Heck coupling synthesis and characterization of a novel tris(4-(pyridine-4-vinyl)phenyl)methylsilane tridentate core, *European Journal of Chemistry*. **15** (2024) 71–73. https://doi.org/10.5155/eurjchem.15.1.71-73.2505.

[26] W.L.A. Brooks, C.C. Deng, B.S. Sumerlin, Structure-Reactivity Relationships in Boronic Acid-Diol Complexation, *ACS Omega*. **3** (2018) 17863–17870. https://doi.org/10.1021/acsomega.8b02999.

[27] X. Kong, J. Ma, S. Garg, T.D. Waite, Tailored Metal–Organic Frameworks for Water Purification: Perfluorinated Fe–MOFs for Enhanced Heterogeneous Catalytic Ozonation, *Environmental Science & Technology*. **58** (2024) 8988–8999. https://doi.org/10.1021/acs.est.4c01133.

[28] T. Viswanathan, N. Palanisami, Ferrocene/non-ferrocene conjugated linear eight-membered borasiloxanes: Structural, theoretical, optical and non-linear optical studies, *Journal of Organometallic Chemistry*. **953** (2021) 122062. https://doi.org/10.1016/J.JORGANCHEM.2021.122062.

[29] O.S. Bull, C. Don-Lawson, Synthesis and crystal structure determination of a new 1D polymer adduct of 1,2-di(pyridin-4-yl) ethane, based on B-N dative bonded eight-membered cyclo-1,33,5,77-hexaphenyl-1,5-dibora-3,7-disiloxane, *European Journal of Chemistry*. **15** (2024) 325–331.

[30] C.D.-L.A.A.A. Okpara Sergeant Bull, Synthesis of an eight-membered 2,2,4,6,6,8-hexaphenyl-1,3,5,7,2,6,4,8- tetraoxadisiladiborocane and its reaction with 4,4-azo-pyridine leading to ring contraction to give a dimer and hydrogen bonded macrocyclic siloxane-azo- pyridine, *European Journal of Chemistry*. **16** (2025) 37–45.

[31] O.S. Bull, E. Okpa, Application of Green Chemistry for the One-pot Preparation of Tris (4-bromophenyl) Chlorosilane, *International Journal of Applied Chemistry*. **10** (2023) 1–5. https://doi.org/10.14445/23939133/ijac-v10i2p101.

[32] Z. Shao, L. Ding, W. Zhu, C. Fan, K. Di, R. Yuan, K. Wang, Highly selective detection and removal of mercury ions in the aquatic environment based on magnetic ZIF-71 multifunctional composites with sufficient chlorine functional groups, *Science of The Total Environment*. **921** (2024) 171085. https://doi.org/https://doi.org/10.1016/j.scitotenv.2024.171085.

[33] F. Rouquerol, J. Rouquerol, K.S.W. Sing, P. Llewellyn, G. Maurin, J. Rouquerol, K.S.W. Sing, P. Llewellyn, 11 – Adsorption by Metal Oxides, in: Adsorption by Powders and Porous Solids, 2014: pp. 393–465. https://doi.org/10.1016/B978-0-08-097035-6.00011-5.

[34] S.E. Wenzel, M. Fischer, F. Hoffmann, M. Fröba, Highly porous metal-organic framework containing a novel organosilicon linker-a promising material for hydrogen storage, *Inorganic Chemistry*. **48** (2009) 6559–6565. https://doi.org/10.1021/ic900478z.

[35] A.B.D. Nandiyanto, R. Ragadhita, J. Yunas, Adsorption isotherm of densed monoclinic tungsten trioxide nanoparticles, *Sains Malaysiana*. **49** (2020) 2881–2890. https://doi.org/10.17576/jsm-2020-4912-01.

[36] A.S.. A.S.N.K.K.G.M.V.T.M.V.T.V.P.B. Sergey V. Baykov; Mikherdov, π–π Noncovalent Interaction Involving 1,2,4- and 1,3,4-Oxadiazole Systems: The Combined Experimental, Theoretical, and Database Study, *Molecules*. **26** (2021) 5672–5686. https://doi.org/10.3390/molecules26185672.

[37] S.M. Hiremath, C.S. Hiremath, S.S. Khemalapure, N.R. Patil, An experimental and theoretical study of molecular structure and vibrational spectra of 2-methylphenyl boronic acid by density functional theory calculations, *AIP Conference Proceedings*. **1953** (2018) 140025. https://doi.org/10.1063/1.5033200.

[38] L. Shi, J. Shi, J. Li, Metabolites changes in inclined stem, *BioResources*. **7** (2012) 3463–3475.

[39] M. Gopalakrishnan, K. Thirumoorthy, N.S.P. Bhuvanesh, N. Palanisami, Eight membered cyclic-borasiloxanes: synthesis, structural, photophysical, steric strain and DFT calculations†, *RSC Advances*. **6** (2016) 55698–55709. https://doi.org/10.1039/C6RA02080A.

[40] T. Viswanathan, M. Gopalakrishnan, K. Thirumoorthy, M. Prakash, N. Palanisami, Enhancement of Second-Order Nonlinear Optical Properties of Centrosymmetric Ferrocenyl Borasiloxane by a Broken-Symmetry Approach, *The Journal of Physical Chemistry C*. **125** (2021) 8732–8740. https://doi.org/10.1021/acs.jpcc.0c11242.

[41] Y. Kawano, Y. Ito, S. Ito, K. Tanaka, Y. Chujo, π-Conjugated Copolymers Composed of Boron Formazanate and Their Application for a Wavelength Converter to Near-Infrared Light, *Macromolecules*. **54** (2021) 1934–1942.

https://doi.org/10.1021/ACS.MACROMOL.0C02315.

[42] O.S. Bull, Solvothermal synthesis and characterization of a new 3D potassium Metal-Organic Framework (MOF) structure, *Journal of the Chemical Society of Nigeria*. **45** (2020) 126–134.

[43] O.S. Bull, C. Don-Lawson, N.-M. Ugo, Synthesis and characterization of a novel eight-membered cyclo-1,3,3,5,7,7- hexaphenyl-1,5-dibora-3,7-disiloxane and 4,4'-bipyridine, 1D adduct, *European Journal of Chemistry*. **15** (2024) 232–238. https://doi.org/10.5155/eurjchem.15.3.232.

[44] S. Bbumba, I. Karume, An Insight into Isotherm Models in Physical Characterization of Adsorption Studies, *Advances in Image and Video Processing*. **12** (2024) 115–134. https://doi.org/10.14738/aivp.122.16738.

[45] M. Musah, Y. Azeh, J. Mathew, M. Umar, Z. Abdulhamid, A. Muhammad, Adsorption Kinetics and Isotherm Models: A Review, *Caliphate Journal of Science and Technology*. **4** (2022) 20–26. https://doi.org/10.4314/cajost.v4i1.3.

[46] M. Gopalakrishnan, T. Viswanathan, E. David, K. Thirumoorthy, N.S.P. Bhuvanesh, N. Palanisami, Second-order nonlinear optical properties of eight-membered centrosymmetric cyclic borasiloxanes, *New Journal of Chemistry*. **43** (2019) 10948–10958. https://doi.org/10.1039/c9nj01611b.

[47] P. Purushothaman, D. Mohanapriya, K. Thenmozhi, S. Karpagam, Designing a ferrocene biphenyl pyridine modified electrode for the non-enzymatic electrochemical detection of catechol, *New J. Chem.* **48** (2024) 6893–6901. https://doi.org/10.1039/D4NJ00710G.